Science Press

ARTICLE

Effect of Y Doping and Vacuum Hot-Press Sintering on Microstructure and Mechanical Properties of TiAl-based Alloys

Li Yang,   Sun Hongliang,   Yang Kang,   Deng Peng,   Chen Zhiyuan

Southwest Jiaotong University, Chengdu 610031, China

Abstract: Ti-45Al and Ti-45Al-0.3Y (at%) samples were fabricated by vacuum hot-press sintering (VHPS). The influence of Y addition and VHPS process parameters on the microstructure and mechanical properties of TiAl-based alloys were analyzed using X-ray diffraction (XRD), optical microscopy (OM), back-scattered electron (BSE) imaging, compression and hardness testing. The results show that optimized sintering parameters are 42 MPa at 1400 °C with holding time of 90 min. Samples prepared under optimized conditions have uniform and fine grains and duplex microstructure consisting of γ phase and $\gamma+\alpha_2$ lamellar colonies. The reaction between γ-TiAl and α_2-Ti$_3$Al reaches completion at a hot-press temperature of 1400 °C for a holding time of 240 min, while significant grain growth occurs under these conditions. The addition of Y has an obvious effect on the refinement of grain and interlamellar spacing, which contributes to an increased mechanical strength of the alloy.

Key words: vacuum hot pressing; Y doping; microstructure; mechanical properties

Because of their outstanding mechanical properties, TiAl-based alloys are considered as the most promising high-temperature structural materials. However, the effect of macro segregation during casting on TiAl-based alloys restricts their use. The high-atomic-number elements tend to sink at the bottom of the ingot, and the low-atomic-number elements float to the top[1-6]. Powder metallurgy (PM) is a favorable process for synthesizing ultrafine-grained and nanostructured TiAl-based alloys, which also helps to solve macro-segregation problem and to form near-net shaped components. Zhang et al[8] has done research on the synthesis of Ti-47Al-2Cr-0.2Mo alloy using plasma rotating electrode process (PREP) and hot isostatic pressing (HIP)[7]. The raw material was Ti-47Al-2Cr-0.2Mo powder. Vacuum hot-press sintering (VHPS) was used by Li et al[8], for fabricating Nb-15W and Nb-15W-10Cr (at%) alloys under 30 MPa for 60 min at 1800 °C in pure argon atmosphere. Sun et al[9] reported the PM of Ti-45Al-10Nb. The alloy was processed by elemental powder metallurgy (EPM) and reactive sintering.

Commercial powders of Ti, Al, and Nb were used as raw materials. Studies have shown that rare-earths Y and Er as additives can result in beneficial or detrimental effects, depending on test conditions, fabrication process, micro-structures, and other factors[10-14]. Xiao et al[15] have done some studies about the effect of Y addition on TiAl-based alloys prepared by SPS (spark plasma sintering). In their work, the TiAl-based alloy was doped with 0.225% Y. Li[16] and Chen[17] have done researches about the effect of Y addition on TiAl-based alloys fabricated by the cast method.

Most of the researches on TiAl-based alloys with Y doping were focused on casting and forging, with little work on powder metallurgy. The objective of this study was to explore the influence of 0.3% Y doping on a TiAl-based alloy by VHPS and to determine the effect of processing parameters on the microstructure and mechanical properties. TiAl-based alloys doped with Y prepared by the PM method were expected to be applied in aerospace sector.

1 Experiment

In this research, the PM method was used. TiAl-based alloy samples were prepared by VHPS, and the raw materials were pure aluminum powder (Al powder), pure titanium hydride powder (TiH_2 powder), and pure yttrium hydride powder (YH_2 powder). The powders were mixed using a planetary boll milling method. The ball mill jar is made of a polyurethane with agate balls. The ball-to-powder mass ratio was 10 to 1. The milling medium was tertiary butanol, the ball-milling time was 4 h, and the rotation speed was 200 r/min. Fig.1 shows the XRD pattern of the original powder. Oxidation was avoided using the hydride powders. The milled slurry was freeze-dried in vacuum for 24 h.

Sample blocks were prepared by VHPS. For all samples, the heating rate was 10 °C/min. There were three parameters for the preparation of the Ti45Al and Ti45Al0.3Y alloys. For a holding temperature of 1345 °C, the holding time was 30 min at a pressure of 30 MPa. For a holding temperature of 1400 °C, two holding time of 90 and 240 min at 42 MPa was used. All the samples were subsequently furnace cooled for 14 h. The vacuum was 1×10^{-4} Pa. Table 1 summarizes the different process conditions for each alloy. Fig.2 is a photograph of the six samples described in Table 1. The diameter of each sample is about 30 mm.

The samples for XRD, metallography, back scattering electron (BSE) imaging, hardness tests, and compression tests were obtained by electric spark-pulse wire cutting. The phases of the TiAl-based alloy were characterized by XRD. Optical
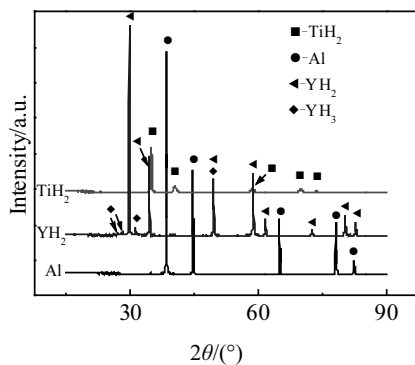

Fig.2   TiAl-based alloy VHPS samples under different conditions described in Table 1

microscopy (OM) and BSE imaging were used to investigate the size and distribution of the different phases in the alloy. A Vickers hardness tester was used to measure the hardness of the alloys, and the room temperature compression and high temperature compression were tested using a universal testing machine. The hardness values of each sample were an average of more than 30 points. The compression-test samples were 6 mm in diameter and 11 mm in thickness.

2 Result and Discussion

2.1 Microstructure and phases

Table 2 shows the density of Ti45Al-XY(X=0, 0.3, at%) alloy prepared by different VHPS processes. The density of TiAl-based alloy is higher than 3.89 g/cm^3, and the relative density of the alloy reaches about 98%. Ti45Al and Ti45Al0.3Y alloy have the highest density when holding temperature is 1400 °C.

Fig.3a shows the XRD patterns of the three Ti45Al-alloy samples processed under different VHPS parameters, with different phases indicated in the patterns. There are only two phases in Ti45Al-alloy samples, γ-TiAl and α_2-Ti$_3$Al, in any sintering conditions. For the higher one of the two sintering temperatures and holding time, the peak intensities of α_2-Ti$_3$Al are higher than those of γ-TiAl, confirming the phase transformation of γ-TiAl to α_2-Ti$_3$Al. This result is consistent with the optical micrographs in Fig.4 and 5. As shown in Fig.3b, the Ti45Al0.3Y alloy is primarily composed of γ-TiAl, α_2-Ti$_3$Al, YAl$_2$, and Y$_2$O$_3$ phases, and the same phase transformation is shown in Fig.3a. Chen et al [17] reported that adding Y to TiAl alloys results in the formation of YAl$_2$, but diffraction peaks of the YAl$_2$ phase are not visible. The reason for the absence of Y$_2$O$_3$ phase is attributed to its low content,

Fig.1   XRD patterns of the original powder

Table 1   VHPS parameters of TiAl-based alloy samples

Sample		Heating rate/ °C·min^{-1}	Holding temperature/°C	Holding time/min	Pressure/ MPa
	1#	10	1345	30	30
Ti45Al	2#	10	1400	90	42
	3#	10	1400	240	42
	4#	10	1345	30	30
Ti45Al0.3Y	5#	10	1400	90	42
	6#	10	1400	240	42

Table 2   Density and relative density of Ti45Al-XY (X=0, 0.3) alloy samples prepared under different VHPS parameters

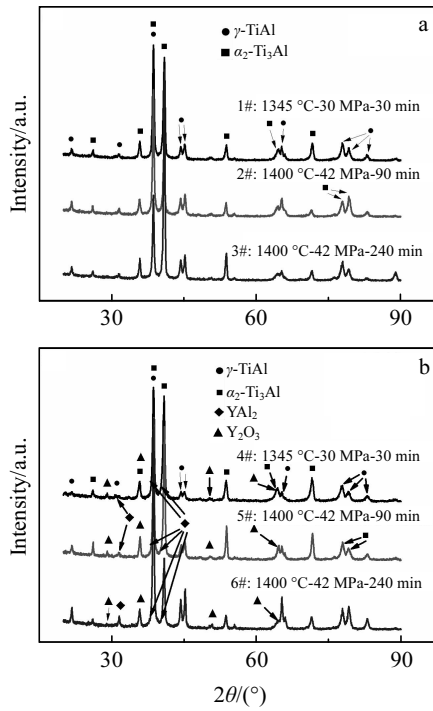| Samples	Density/g·cm^{-3}	Relative density/%
1#	3.8931	98.41
2#	3.9201	99.10
3#	3.9169	99.01
4#	3.9101	98.84
5#	3.9226	99.16
6#	3.9203	99.10

Fig.3   XRD patterns of Ti45Al (a) and Ti45Al0.3Y (b) under different VHPS parameters

so it was not detectable by XRD.

Fig.4 and Fig.5 show the OM images of TiAl-based alloys with different VHPS parameters. Prolonged holding time and higher temperature of 1400 °C caused the transformation from α_2-Ti$_3$Al to equiaxed γ-TiAl, resulting in the formation of a lamellar microstructure. However, some equiaxed γ-TiAl phases were still present in the samples treated at lower temperature. In Fig.4, excessive grain growth occurs due to the prolonged holding time and the higher pressing temperature. In particular, in Fig.4c, the grain diameter increased to hundreds of microns. Large grains resulted in inferior mechanical properties. Fig.5 shows the grain structures of Ti45Al0.3Y samples under different VHPS processes. At 1350 and 1400 °C, for 90 min, the grain sizes were large, but they were still smaller than those of Ti45Al without Y. Average grain size was 40 μm. The addition of Y to the alloy resulted in grain refinement. Presence of the YAl$_2$ and Y$_2$O$_3$ phases resulted in grain boundary pinning, which hindered coarsening; the presence of these phases at the grain boundaries prevented the movement of dislocations. As shown in Fig.5c, the grain diameter is about 70~100 μm. However, Fig.5b shows a better result; the grain size is restricted to 40 μm at 1400 °C for 90 min. Suardi et al[18] reported that the as-cast Ti45Al held at 1200 °C developed coarse grains of about 200 μm. The YAl$_2$ and Y$_2$O$_3$ phases could not be observed under the optical microscope, so BSE image was used, as shown in Fig.6.
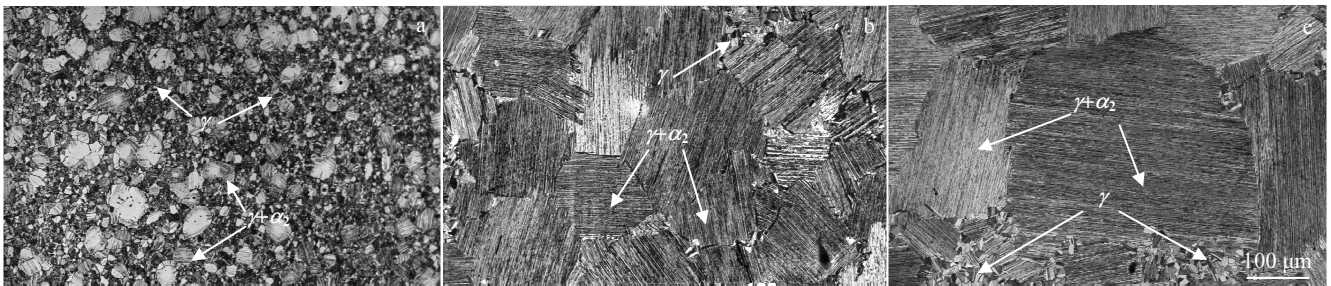

Fig.4   OM images of Ti45Al alloy processed under different VHPS parameters: (a) 1# 1345 °C-30 MPa-30 min; (b) 2# 1400 °C-42 MPa-90 min; (c) 3# 1400 °C-42 MPa-240 min
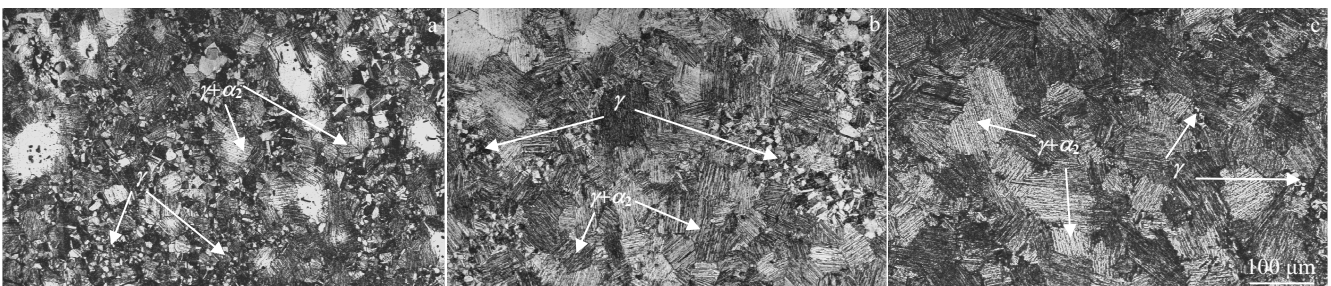

Fig.5   OM images of Ti45Al0.3Y alloy processed under different VHPS process parameters: (a) 4# 1345 °C-30 MPa-30 min; (b) 5# 1400 °C-42 MPa-90 min; (c) 6# 1400 °C-42 MPa-240 min

Fig.6 shows BSE images of samples 2# and 5# processed at 1400 °C for 90 min at a pressure of 42 MPa. In Fig.6a and 6b, regions of pure γ phase as well as $\gamma+\alpha_2$ are illustrated. In addition, according to the EDS data shown in the inset of Fig.6b and the XRD pattern in Fig.3b, the light gray areas in Fig.6b are YAl_2 and Y_2O_3 phases. Because the Y_2O_3 and YAl_2 phases have a lighter color in the BSE image, they cannot be distinguished. The light phase (Y_2O_3 and YAl_2 phases) in Ti45Al0.3Y alloy accounts for 0.98% (±0.24) of total area of the alloy. The average size of the light phase was 0.2~2 μm. However, an unusually large size exceeding 10 μm was observed. It was harmful to the mechanical properties of alloy. YAl_2 and Y_2O_3 phases in Fig.6b and 6d are marked by arrows as Y-rich. In the hot-press sintering process, Y first combined with O in the matrix to form Y_2O_3, and then the extra Y and Al formed YAl_2. These Y_2O_3 and YAl_2 phases were mainly distributed in the grain boundary. At 1400 °C, the phases entered the single α-phase region and increased rapidly. Since these Y-rich phases were pinned at the grain boundaries, the growth of the α-phase was hindered, thereby refining the grains. Although the large-sized Y-rich phase was located at the grain boundary, many smaller size phases were distributed between the layers. When the γ phase was precipitated from the α_2 phase, these small Y-rich phase can increase the nucleation rate and promote the precipitation of γ phase from the α_2 phase, refining the lamellar. In Fig.6d, there are many places exhibiting signs of γ precipitated from the α_2 phase. In fact, this is the result of the refinement of lamellar structure. Fig.6c shows the lamellar structure of alloy without Y, and no phenomenon of lamellar refinement is found, so the lamellar spacing is larger. The refinement of the grains and the reduction of the interlamellar spacing are beneficial to the hardness and compression resistance of the material, which is verified in the mechanical performance analysis below.

2.2 Mechanical properties

Table 3 shows the hardness and compressive strength values of the two TiAl-based alloys. As shown in Table 3, samples 1# and 4# undergo the same VHPS process, but the average hardness of 4# is higher than that of 1#. The other two comparison data of 2# to 5# and 3# to 6# show the same results. These results indicate that the hardness of TiAl-based alloys can be improved by adding the rare earth element Y. The addition of Y can result in the formation of the YAl_2 and Y_2O_3 phases, and these phases are distributed around the grain periphery and prevent the extension of the grain boundary, resulting in finer grains. According to Hall-Petch formula, the smaller the grain size, the better the strengthen effect, and the higher the hardness of the alloy. It was also found that TiAl-based alloys with the same component processed under different VHPS conditions exhibit different hardness values. Among the three used holding time of 30, 90, and 240 min and the two temperatures of 1345 and 1400 °C, the highest hardness was obtained at 1400 °C for 90 min. The hardness was lowest when the holding time was 240 min at the same sintering temperature. The reason is that for TiAl alloys, the hardness of the alloy is not only affected by the grain size but also by the microstructure. In general, the hardness of the lamellar structure is higher than that of the γ microstructure, so the hardness of the sample 5# is higher than that of the sample 4# due to the formation of more lamellar structures. The hardness of the sample 6# was lower than that of the samples 4# and 5# due to the larger grain.

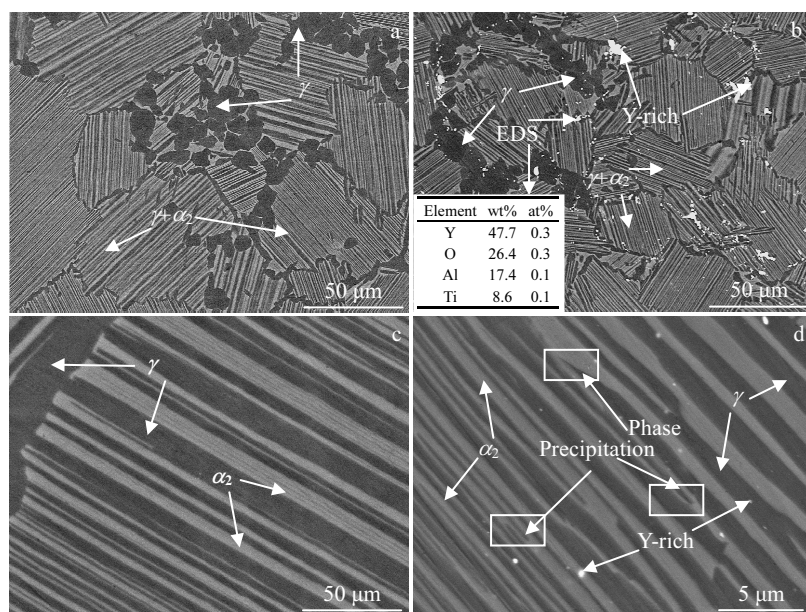| Element	wt%	at%
Y	47.7	0.3
O	26.4	0.3
Al	17.4	0.1
Ti	8.6	0.1

Fig.6   BSE images of the TiAl-based alloy processed at 1400 °C for 90 min: (a, c) sample 2# and (b, d) sample 5#

Table 3 and Fig.7 show the compression value and curve of the two-component TiAl-based alloys processed under different VHPS processes, respectively. Each sample was subjected to two compression tests. According to the average compressive strength of each sample, it can be concluded that the compressive strength of the sample in Fig.7b is significantly higher than that of the sample in Fig.7a. This result can also be found in Table 3. Table 3 lists a compressive value of as-cast Ti45Al [19]. The strain of as-cast Ti45Al is lower than that of the PM Ti45Al alloy and is significantly lower than that of PM Ti45Al0.3Y. This is because the Y addition ensures the grain refinement of the alloy and can absorb the oxygen from the matrix, and the formed Y-rich phase acts as an effect of dispersion-strengthening, so that the compressive strength is improved. Moreover, with the prolongation of holding time, the lamellar microstructure of the grains was finer and more prevalent. This has an effect of distributing pressure, and then the toughness of the alloy is improved. From Fig.7, the strain of the curve in Fig.7b is higher than that in Fig.7a. This is not only due to the effect of the grain refinement but also as a result of an increase in the number of lamellar structures in the grains. Table 3 also lists the high temperature compression properties of the material. The compressive strength at 700 °C and room temperature are very close, which is an obvious characteristic of the intermetallic compounds. In summary, the addition of Y can improve the hardness and compressive strength of TiAl-based alloys.

Table 3   Hardness and compressive strength of Ti45Al and Ti45Al0.3Y processed with different VHPS processes

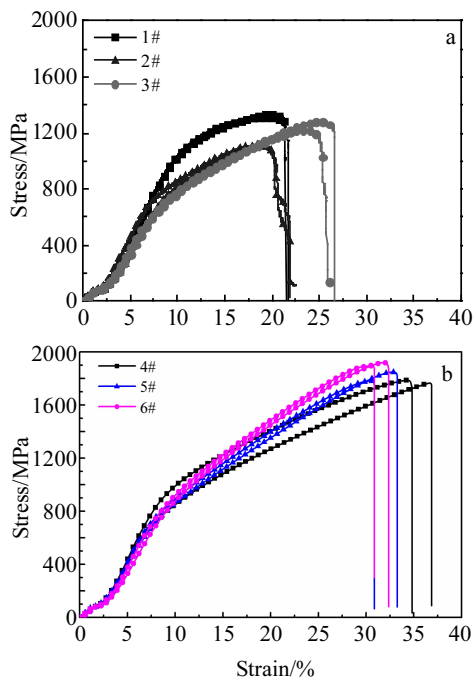| Sample	Hardness/×10 MPa	Compressive strength/MPa	Final strain/%	High temperature compressive strength (700 °C)/MPa
1#	337(±18)	1310	21.7	1278
2#	362(±21)	1110	22	1211
3#	330(±24)	1243	26.9	1134
4#	358(±14)	1765	35	1888
5#	379(±18)	1797	32.7	1801
6#	344(±25)	1875	32.4	1812
As-cast Ti45Al	-	1781 [19]	16.2 [19]	-

Fig.7   Compression curves of Ti45Al (a) and Ti45Al0.3Y(b) alloys processed under different VHPS conditions

3   Conclusions

1) Ti45Al and Ti45Al0.3Y can be fabricated using Al powder, TiH$_2$ powder, and YH$_2$ powder by VHPS process. γ-TiAl and α$_2$-Ti$_3$Al can be found in Ti45Al.

2) YAl$_2$ and Y$_2$O$_3$ phases appear in Ti45Al0.3Y, which only play a role of dispersion strengthening, but also refine the grain and lamellar spacing. The grain size of alloys with Y addition can be refined to 40 μm at 1400 °C for 90 min. Under this condition, TiAl alloy has the highest mechanical properties.

References

1   Brady M P, Wright I G, Gleeson B. *JOM*[J], 2000, 52(1): 16
2   Kim Y W. *Acta Metall Mater*[J], 1992, 40(6): 1121
3   Clemens H, Kestler H. *Mater*[J], 2000, 2(9): 551
4   Yang C, Hu D, Huang A *et al*. *Intermetallics*[J], 2013, 32: 64
5   Yang C, Jiang H, Hu D *et al*. *Scripta Materialia*[J], 2012, 67(1): 85
6   Hu D, Yang C, Huang A *et al*. *Intermetallics*[J], 2012, 22: 68
7   Zhang D Y, Li H Z, Liang X P *et al*. *Materials and Design*[J], 2014, 59: 415
8   Li B, Zhang K. *Vacuum*[J], 2012, 86(9): 1341
9   Sun H F, Li X W, Fang W B. *Trans Nonferrous Met Soc China*[J], 2015, 25(5): 1454

10 Bennett M J, Bishop H E, Chalker P R *et al. Mater Sci Eng A*[J], 1987, 90: 177

11 Jung H G, Wee D M, Oh M H. *Oxid Met*[J], 1998, 49(5): 403

12 Huntz A M, Zhao J G. *Mater Sci Eng A*[J], 1987, 88: 213

13 Khanna A S, Wasserfuhr C, Quadakkers W J. *Mater Sci Eng A*[J], 1989, 120(1): 129

14 Tsai S C, Huntz A M, Dolin C. *Oxid Met*[J], 1995, 43(5): 581

15 Xiao S L, Xu L J, Yu H B *et al. Rare Metal Materials and Engineering*[J], 2013, 42(1): 23

16 Li B H, Kong F T, Chen Y Y. *Journal of Rare Earths*[J], 2006, 24(3): 352

17 Chen Yuyong, Li Baohui, Kong Fantao. *Rare Metal Materials and Engineering*[J], 2006, 35(1): 1

18 Suardi K, Hamzah E, Ourdjini A *et al. Journal of Materials Processing Technology*[J], 2007, 185 (1-3): 106

19 Morris M A, Li Y G, Leboeuf M. *Scripta Metallurgica et Materialia*[J], 1994, 31(4): 449

Y 掺杂及真空热压烧结对 TiAl 基合金显微组织和力学性能的影响

李　阳，孙红亮，杨　康，邓　鹏，陈志元

(西南交通大学，四川 成都 610031)

摘　要：Ti-45Al 和 Ti-45Al-0.3Y（at%）样品通过真空热压烧结的方法制备。样品通过 X 射线衍射（XRD）、光学显微镜（OM）、背散射电子成像（BSE）以及压缩和硬度测试来研究 Y 掺杂和热压工艺参数对 TiAl 基合金的显微组织和力学性能的影响。 结果表明，最优烧结参数为压力 42 MPa，1400 ℃下保温保压 90 min。在此参数下，得到了组织均匀、晶粒细小的由 γ 相和 $\gamma+\alpha_2$ 片层结构组成的双态组织。在热压温度 1400 ℃，保温时间 240 min 下，反应充分但会出现晶粒粗大现象。Y 的加入对细化晶粒和片层间距有明显的影响，这有助于提高合金的机械强度。

关键词：真空热压烧结；Y 掺杂；显微组织；力学性能

作者简介：李　阳，男，1989 年生，硕士生，西南交通大学材料科学与工程学院，四川 成都 610031，电话：028-87634177，E-mail: 1354944342@qq.com